

Induction of Oxidative Stress in *Trypanosoma brucei* by the Antitrypanosomal Dihydroquinoline OSU-40

Shanshan He,^a Alex Dayton,^b Periannan Kuppasamy,^b Karl A. Werbovetz,^a and Mark E. Drew^{a,c}

Division of Medicinal Chemistry and Pharmacognosy, College of Pharmacy, The Ohio State University, Columbus, Ohio, USA^a; Department of Internal Medicine, Davis Heart and Lung Research Institute, The Ohio State University, Columbus, Ohio, USA^b; and Department of Microbial Infection and Immunity, College of Medicine, The Ohio State University, Columbus, Ohio, USA^c

Dihydroquinoline derivative OSU-40 (1-benzyl-1,2-dihydro-2,2,4-trimethylquinolin-6-yl acetate) is selectively potent against *Trypanosoma brucei rhodesiense* *in vitro* (50% inhibitory concentration [IC₅₀], 14 nM; selectivity index, 1,700) and has been proposed to cause the formation of reactive oxygen species (ROS) in African trypanosomes (J. Fotie et al., *J. Med. Chem.* 53:966–982, 2010). In the present study, we sought to provide further support for the hypothesis that OSU-40 kills trypanosomes through oxidative stress. Inducible RNA interference (RNAi) was applied to downregulate key enzymes in parasite antioxidant defense, including *T. brucei* trypanothione synthetase (TbTryS) and superoxide dismutase B (TbSODB). Both TbTryS RNAi-induced and TbSODB RNAi-induced cells showed impaired growth and increased sensitivity toward OSU-40 by 2.4-fold and 3.4-fold, respectively. Decreased expression of key parasite antioxidant enzymes was thus associated with increased sensitivity to OSU-40, consistent with the hypothesis that OSU-40 acts through oxidative stress. Finally, the dose-dependent formation of free radicals was observed after incubation of *T. brucei* with OSU-40 utilizing electron spin resonance (ESR) spectroscopy. These data support the notion that the mode of antitrypanosomal action for this class of compounds is to induce oxidative stress.

Human African trypanosomiasis (HAT) is a vector-borne parasitic disease caused by the *Trypanosoma brucei* subspecies *T. b. rhodesiense* and *T. b. gambiense*. The trypanosome proliferates in the host's hemolymphatic system during the first stage of HAT and invades the central nervous system in the second stage. Transmitted by the tsetse fly, the disease mainly affects rural populations in sub-Saharan Africa and is fatal if untreated. Although according to the World Health Organization the number of new cases has dropped to just over 7,000 during 2010 (39), very few drugs are available to treat HAT (2, 4, 42). Pentamidine and suramin, both developed in the first half of the 20th century, are used against first-stage disease, while melarsoprol and eflornithine are used to treat second-stage disease. These drugs are far from satisfactory due to limitations such as severe toxicity, poor efficacy, acquired resistance, rising failure rates, and lack of availability (2, 4, 42). With high efficacy and a good safety profile, nifurtimox-eflornithine combination therapy (NECT) was introduced as a first-line treatment for second-stage HAT caused by *T. b. gambiense* in 2009 (4, 22, 42). However, administration of NECT is relatively complicated, and its efficacy toward *T. b. rhodesiense* is still questionable (4, 42). Thus, new drugs are needed against HAT that are safe, affordable, easy to administer, active against first- and second-stage disease, and effective against both subspecies of *T. brucei* (4, 42).

From a previous synthetic medicinal chemistry study, we discovered several N1-substituted 1,2-dihydroquinoline-6-ols displaying nanomolar 50% inhibitory concentrations (IC₅₀s) *in vitro* against *T. b. rhodesiense* and selectivity indexes (SI) up to >18,000 (11). OSU-40 (1-benzyl-1,2-dihydro-2,2,4-trimethylquinolin-6-yl acetate) (Fig. 1) showed a potency (IC₅₀, 0.014 μM; SI, 1,700) close to that of melarsoprol (IC₅₀, 0.008 μM; SI, 1,000) against *T. b. rhodesiense* STIB900 *in vitro*. In an early treatment mouse model of acute African trypanosomiasis, OSU-40 prolonged the life span of infected mice when given intraperitoneally (i.p.) at 50 mg/kg/day for 4 consecutive days (>14 days versus 7.75 days for untreated controls). A

subsequent study showed that three closely related dihydroquinolines provided cures in a murine model of African trypanosomiasis when given i.p. at 50 mg/kg/day for 4 days (29). The following observations pointed to ROS generation as a mechanism to account for the antitrypanosomal activity of the dihydroquinolin-6-ols. First, SAR studies suggested that only dihydroquinolines capable of forming a quinone imine species through bioactivation displayed potent *in vitro* antitrypanosomal activity (11). Second, an experiment using the redox-sensitive dye CM-H₂DCFDA was consistent with the hypothesis that ROS were produced in the parasites dose dependently when *T. b. brucei* was exposed to OSU-40 *in vitro* (11).

In this study, we used OSU-40 to further investigate the mode of action of these promising dihydroquinolines. From both indirect evidence from RNA interference (RNAi) of enzymes involved in parasite antioxidant defense and direct evidence provided by electron spin resonance (ESR) spectroscopy, we conclude that OSU-40 induces oxidative stress. These studies further establish the mode of action of the dihydroquinolines and suggest the induction of oxidative stress as a promising target for anti-HAT drug development.

MATERIALS AND METHODS

Materials. All chemicals were purchased from Sigma-Aldrich Chemical Co., unless stated otherwise. OSU-40 was synthesized following the procedure of Fotie et al. (11).

Received 16 December 2011 Returned for modification 5 January 2012

Accepted 25 January 2012

Published ahead of print 6 February 2012

Address correspondence to Mark E. Drew, mark.drew@osumc.edu.

Copyright © 2012, American Society for Microbiology. All Rights Reserved.

doi:10.1128/AAC.06386-11

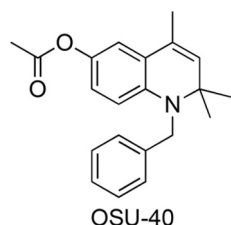


FIG 1 Chemical structure of OSU-40.

Trypanosome culture. Bloodstream form *T. brucei brucei* strain 221 and transgenic cell line 90-13 (a gift from James Morris, Clemson University, SC) were cultured at 37°C under 5% CO₂ in HMI-9 medium (14) supplemented with 20% fetal bovine serum. 90-13 cells were supplemented with 2.5 μg/ml G418 and 5 μg/ml hygromycin.

Generation of RNAi constructs. Fragments of the *T. brucei* genes encoding trypanothione synthetase (TbTryS) and superoxide dismutase B (TbSODB) were amplified by PCR from *T. b. brucei* 90-13 genomic DNA (see Table 1 for primer sequences), digested with HindIII and XhoI, and cloned into the pZJMα vector (38), replacing the α-tubulin stuffer region, and transformed into *Escherichia coli* DH5α competent cells (Invitrogen, Carlsbad, CA). Plasmid DNA was purified using a DNA maxiprep kit (Qiagen, Valencia, CA), and inserts were verified by DNA sequencing. Prior to transfection, the plasmids pZJMα-TbTRYs and pZJMα-TbSODB were linearized by digestion with NotI.

Transfection of the parent cell line. Bloodstream form parental 90-13 cells were transfected with the Nucleofector system (Lonza, Basel, Switzerland). A total of 1.5×10^7 to 3×10^7 cells at mid-log phase (culture density, 3×10^5 to 6×10^5 cells/ml) were resuspended in 100 μl of freshly made human T-cell Nucleofector solution, mixed with 5 μg of the desired linearized pZJMα construct, and subjected to nucleofection employing program X-001 (3). Immediately after transfection, cells were transferred into 75 ml of prewarmed medium and incubated overnight for recovery at 37°C under 5% CO₂. Selection was achieved by the addition of 2.5 μg/ml phleomycin. For controls, the same procedure was conducted without DNA. Resistant clones were evident after approximately 10 days and transferred to culture flasks. Clonal cells were obtained by limiting dilution.

Phenotype growth inhibition. Bloodstream form trypanosomes transfected with each of the RNAi constructs were maintained at cell densities from 1×10^5 to 5×10^6 cells/ml at 37°C in the presence or absence of 1 μg/ml tetracycline. Every 20 to 24 h, aliquots were taken from cell culture and parasite growth was assessed microscopically. Cumulative cell density was obtained by multiplying the cell density by the overall dilution factor at each time point.

qRT-PCR. Approximately 0.5×10^7 to 1×10^7 cells were collected 3 days after the induction of RNAi, and RNA was isolated using the RNeasy minikit (Qiagen, Valencia, CA). Residual DNA was removed using the TURBO DNA-free kit (Applied Biosystems, Carlsbad, CA). cDNA was synthesized using the iScript cDNA synthesis kit (Bio-Rad, Hercules, CA). Quantitative real-time PCR (qRT-PCR) was performed using iQ SYBR green supermix (Bio-Rad, Hercules, CA) in a Bio-Rad CFX96 real-time PCR system (initial

denaturation at 94°C for 3 min, followed by 40 cycles of denaturation at 94°C for 10 s and annealing and extension at 57°C for 30 s). All reactions were normalized to trypanosome β-actin (TbActin). Relative mRNA expression was analyzed using the cycle threshold ($2^{-\Delta\Delta CT}$) method (20). Primer sequences for TbTryS and TbActin are shown in Table 1.

Western blotting. All steps were carried out at room temperature unless otherwise noted. Approximately 1×10^7 to 1.5×10^7 cells were pelleted by centrifugation at $800 \times g$ for 10 min and lysed in 30 to 50 μl of lysis buffer containing 50 mM Tris-HCl (pH 8.1), 1% sodium dodecyl sulfate (SDS), 10 mM EDTA, and SigmaFAST protease inhibitor tablets. Lysates were sonicated for 10 s using a Virtis Virsonic 300 ultrasonic cell disruptor and cooled on ice for 10 s. Cell debris was cleared by centrifugation at $13,200 \times g$ for 15 min at 4°C. Protein concentrations of soluble fractions were measured using a bicinchoninic acid assay (Pierce, Rockford, IL). Lysates were boiled for 10 min following addition of 5× SDS-polyacrylamide gel electrophoresis sample buffer (300 mM Tris-HCl [pH 6.8], 10% SDS, 5% β-mercaptoethanol, 50% glycerol, 0.05% bromophenol blue). Ten micrograms of protein from each lysate was resolved on 10% SDS-polyacrylamide gels and transferred to Amersham Hybond-ECL nitrocellulose membrane (GE Healthcare, Pittsburgh, PA). Membranes were blocked with 5% (wt/vol) nonfat milk in TBST (20 mM Tris-HCl, 150 mM NaCl [pH 7.6], 0.1% Tween 20) for 30 min and washed 3 times for 10 min with TBST prior to incubation with primary antiserum. Rat polyclonal antiserum against recombinant TbTryS (provided by Alan Fairlamb, University of Dundee, United Kingdom) was diluted 1:500 in TBST containing 5% (wt/vol) bovine serum albumin. Rabbit polyclonal antiserum against parasite α-enolase (provided by Paul Michels, Catholic University of Louvain, Brussels, Belgium) was diluted 1:1000 in TBST containing 5% (wt/vol) nonfat milk. The membranes were washed 3 times for 10 min in TBST and incubated with goat anti-rat or anti-rabbit immunoglobulin G-horseradish peroxidase (Jackson ImmunoResearch Laboratories, Inc.) conjugates (1:5,000) for 1 h. Following three 10-min washes with TBST, the proteins were visualized by chemiluminescence with Amersham ECL Western blotting detection reagent (GE Healthcare, United Kingdom).

In vitro susceptibility assay. All incubations were carried out at 37°C in a humidified 5% CO₂ atmosphere, unless otherwise noted. The activity of compounds toward TbTryS RNAi and TbSODB RNAi cell lines were tested in the presence or absence of 1 μg/ml tetracycline following the procedure of Reid et al. (29) with some modifications. Parasite cultures at a starting density of 1×10^5 cells/ml were seeded in 96-well plates in a volume of 100 μl/well with or without test compounds for 72 h. Twenty-five microliters of 3-(4,5-dimethylthiazol-2-yl)-2,5-diphenyltetrazolium bromide (MTT) (5 mg/ml in autoclaved water) was added to each well, followed by an additional 2 h of incubation. One hundred microliters of 10% SDS lysis buffer (prepared in 50% dimethyl formamide) was added to each well, and plates were incubated for 3 to 6 h. A SpectraMax Plus microplate reader (Amersham Biosciences, Piscataway, NJ) was used to measure the optical densities of each well at 570 nm. IC₅₀s were determined with the aid of the software program SoftMax Pro (Amersham Biosciences, Piscataway, NJ), using the dose-response equation $y = \{[a - d]/[1 + (x/c)^b]\} + d$, where x is the drug concentration, y is absorbance at 570 nm, a is the upper asymptote, b is the slope, c is the IC₅₀, and d is the lower asymptote.

TABLE 1 Primer sequences for RNAi constructs and qRT-PCR

Usage	Gene product	Sequence of ^a :	
		Forward primer	Reverse primer
RNAi construct	TbTryS	ctcgagCACGTTCCCTTTGGTGAGAT	aagcttCTCTGCTGCATGATCCTCAA
	TbSODB	ctcgagCAAAGGGCATATCGAAGGAA	aagcttGCTTGAGATCCGCTTCAGTC
qRT-PCR	TbTryS	CCATTGGTGTTCATGAGTC	TGTCAAGTCCAGCCAGTCAG
	TbActin	GCCACGTATTTCCATCCATC	CCTGAGCTTCATCACCAACA

^a Lowercase letters represent XhoI and HindIII sites.

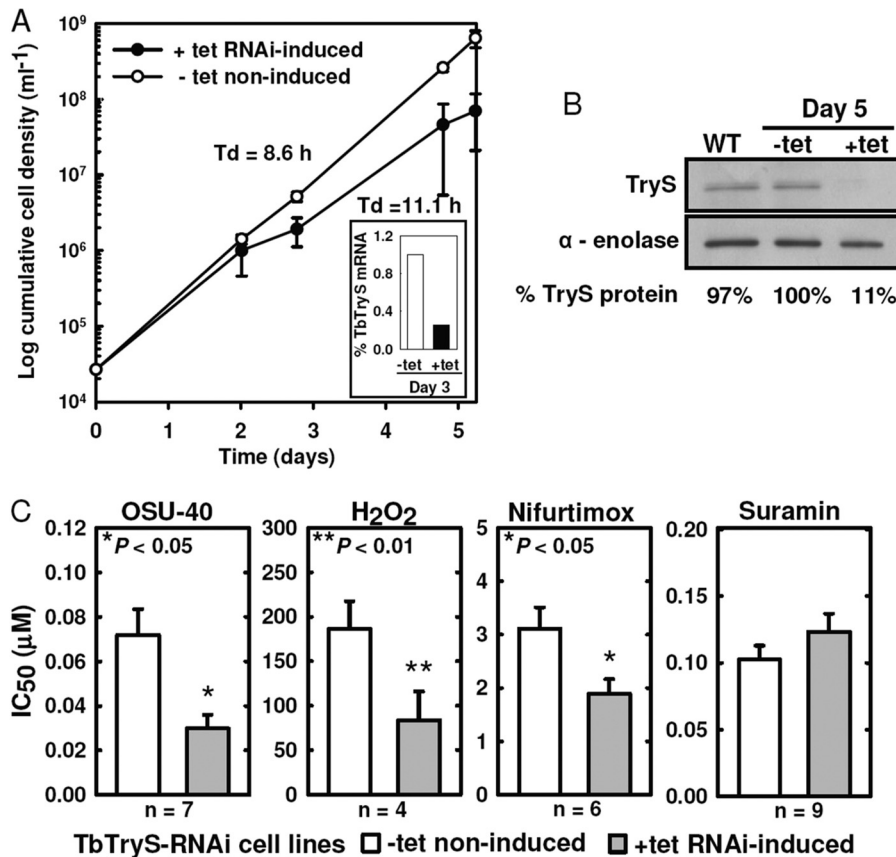


FIG 2 Effect of TbTryS RNAi on bloodstream form parasite growth, TbTryS protein level, and susceptibility to OSU-40. (A) Growth of RNAi-induced (+tet) and noninduced (–tet) TbTryS RNAi cell lines. “Td” indicates the doubling time over 5 days. Results are means \pm standard errors (SE) from three independent experiments. (Inset of panel A) Real-time PCR shows 4-fold-lower TryS mRNA levels in RNAi-induced (+tet) compared to noninduced (–tet) cells collected 3 days after induction. (B) Western blot analysis of TbTryS expression in wild-type (WT) 90-13 and noninduced (–tet) and RNAi-induced (+tet) trypanosomes collected 5 days after induction. %TbTryS indicates protein abundance relative to that in noninduced cells quantified using ImageJ software (public domain; National Institutes of Health) after normalizing to α -enolase bands. The blot is representative of three independent experiments. (C) Susceptibility of RNAi-induced (+tet) and noninduced (–tet) TbTryS RNAi cell lines to OSU-40, H₂O₂, nifurtimox, and suramin. RNAi was initiated and maintained for at least 3 days prior to initiation of the susceptibility assay (see Materials and Methods). The results shown are the means of at least four independent experiments \pm SE (n = the number of independent experiments). Asterisks (*, $P < 0.05$; and **, $P < 0.01$) indicate statistically significant differences in IC₅₀s between RNAi-induced and noninduced cells as assessed by Student’s t test.

ESR. The production of free radicals was detected by ESR spectroscopy after incubation of compounds with bloodstream form *T. b. brucei* strain 221 parasites. Cells in the late log stage were centrifuged at $800 \times g$ for 10 min and resuspended in 50 mM phosphate buffer (pH 7.4) in the presence of 10 mM glucose, 10 mM spin trapping reagent 5-(diethoxyphosphoryl)-5-methyl-1-pyrroline *N*-oxide (DEPMPO), and 10 μ M chelating reagent diethylenetriamine-pentaacetic acid (DETPAC). Stock solutions of the compounds in DMSO were added, after which the suspension was transferred into a 50- μ l capillary tube and incubated for 60 min. ESR spectra were recorded on a Bruker EMX X-band spectrometer system (Bruker Biospin, Billerica, MA) and characterized by computer simulations using Winsim software (Public EPR Software Tools, National Institute of Environmental Health Sciences, Durham, NC).

Statistical analysis. Statistical significance was assessed by Student’s t test using SigmaPlot 10.0 software (Systat Software, Inc., San Jose, CA). Differences were considered significant when P was ≤ 0.05 .

RESULTS

RNAi-mediated knockdown of TbTryS results in reduced TbTryS expression and increased sensitivity toward OSU-40 *in vitro*. To assess the role of TbTryS in *T. brucei* sensitivity to OSU-40, bloodstream form 90-13 cells were transfected with plasmid

pZJM α -TbTRYs. This allows induction of TbTryS RNAi in the presence of tetracycline and consequent reduction in TbTryS expression. In the absence of tetracycline, TbTryS RNAi cells grew at approximately the same rate as the parental 90-13 cells (data not shown). Following the addition of tetracycline for 72 h, a significant reduction in the growth rate of TbTryS RNAi cells was observed with a corresponding 4-fold reduction of endogenous TbTryS mRNA (Fig. 2A). The doubling time increased from 8.6 h to 11.1 h as measured over the first 5 days postinduction, with a cumulative cell density for induced parasites being 11% of that of the noninduced cultures on day 5. Western blot analysis confirmed that the level of TbTryS protein was significantly reduced in TbTryS RNAi-induced cells compared to that in noninduced and wild-type cultures (Fig. 2B). The results described above were consistent with reported effects of TbTryS RNAi on parasite growth and the level of TbTryS protein in *T. brucei* parasites (1, 7).

TbTryS is an essential enzyme in the parasite defense against oxidative stress (1, 7). If the trypanocidal effect of OSU-40 is mediated through extensive oxidative stress, we hypothesized that downregulation of TbTryS should then sensitize the parasites to

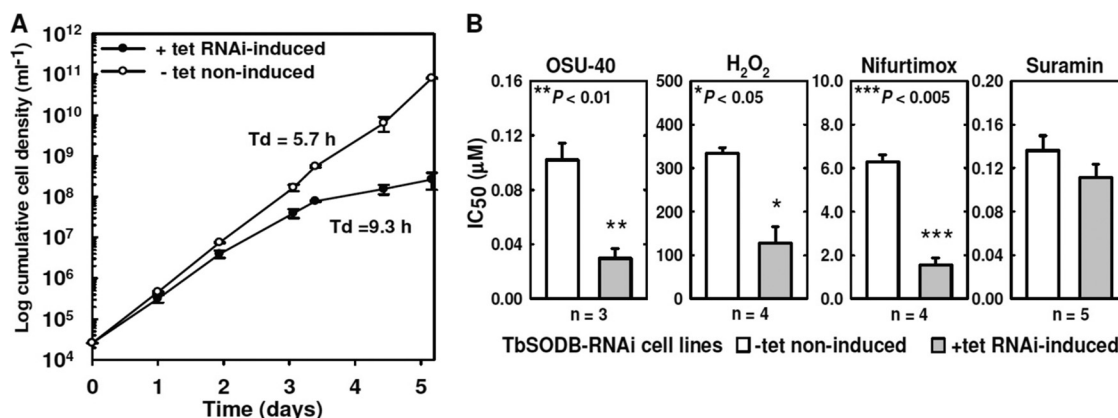


FIG 3 Effect of TbSODB RNAi on bloodstream form parasite growth and susceptibility to OSU-40. (A) Growth of RNAi-induced (+tet) and noninduced (–tet) TbSODB RNAi cell lines. “Td” indicates the doubling time over 5 days. The results are means \pm SE from two independent experiments. (B) Susceptibility of RNAi-induced (+tet) and noninduced (–tet) TbSODB RNAi cell lines to OSU-40, H₂O₂, nifurtimox, and suramin. RNAi was initiated and maintained for at least 2 days prior to susceptibility assays. The results shown are the means of at least three independent experiments \pm SE (n = the number of independent experiments). Asterisks (*, $P < 0.05$; **, $P < 0.01$; and ***, $P < 0.005$) indicate statistically significant differences in IC₅₀s between RNAi-induced and noninduced cells as assessed by Student’s t test.

OSU-40. Consistent with our hypothesis, RNAi-induced bloodstream form trypanosomes were 2.4-fold ($P < 0.05$) more susceptible to OSU-40 as determined by MTT assays of parasite viability (Fig. 2C). H₂O₂, nifurtimox, and suramin were employed as controls. Both H₂O₂ and nifurtimox were reported to show increased activity on trypanosomes with TbTryS knockdown by RNAi (1, 7). Suramin, which served as a negative control for the changes in potency of OSU-40 following TbTryS knockdown, acts through a mechanism not directly related to oxidative stress (2). The potencies of H₂O₂ and nifurtimox both increased on RNAi-induced parasites by 2.2-fold ($P < 0.01$) and 1.6-fold ($P < 0.05$), respectively, while the activity of suramin was unchanged.

RNAi-mediated knockdown of TbSODB increases sensitivity toward OSU-40 in vitro. To further confirm that downregulation of essential trypanosome antioxidant enzymes leads to increased sensitivity to OSU-40, a TbSODB RNAi cell line was also generated. Consistent with previously reported findings (40), RNAi-mediated downregulation of TbSODB led to a dramatic decrease in parasite growth rate (Fig. 3A), with the doubling time lengthened from 5.7 to 9.3 h over the first 5 days after induction and with the cumulative cell density of induced parasites being as low as 0.3% of that of the noninduced cultures on day 5.

The antiparasitic potency of OSU-40 was evaluated in TbSODB RNAi-induced and noninduced parasites, together with H₂O₂, nifurtimox and suramin. Similar to our observation with TbTryS RNAi-induced trypanosomes, parasites with downregulated TbSODB became 3.4-fold ($P < 0.01$) more susceptible to OSU-40. H₂O₂ and nifurtimox were also more active on RNAi-induced parasites (2.6-fold [$P < 0.05$] and 4.1-fold [$P < 0.005$], respectively). At the same time, downregulation of TbSODB did not lead to a significant rise in susceptibility to suramin. This again confirmed that the increased activity of OSU-40 was not a general effect due to the knockdown of TbSODB.

OSU-40 induces free radical formation when incubated with bloodstream form *T. brucei*. Parasites were treated with OSU-40 for 1 h, and the cell suspension was analyzed using ESR spectroscopy. The spin trapping reagent DEPMPO was added to the cell suspension to permit the measurement of short-lived

free radicals. Clearly resolved 12-line spectra were observed after treatment of trypanosomes with both OSU-40 and H₂O₂ (Fig. 4A). Computer simulation was carried out to characterize the ESR spectra obtained after exposure of parasites to 10 μ M OSU-40 for 60 min. The simulation identified the presence of two isomers of DEPMPO adduct with the following coupling constants (G): isomer 1, ³¹P, 47.049, ¹H, 20.033, and ¹⁴N, 14.494; and isomer 2, ³¹P, 46.402, ¹H, 22.398, and ¹⁴N, 14.445. The calculated spectral parameters were in agreement with those of the carbon-centered adduct (36). Similar results were obtained for all of the DEPMPO adducts following exposure of the parasites to OSU-40 and H₂O₂. Induction of free radicals by OSU-40 in bloodstream form *T. brucei* was dose dependent based on quantification of ESR signal amplitudes (Fig. 4B).

DISCUSSION

For drugs and drug candidates, knowledge of their mode of action can direct efforts to improve activity, pharmaceutical properties, and clinical applications. Mode-of-action studies can also shed light on the basis for selectivity and mechanisms of resistance. Understanding the mode of action of a novel series of compounds should also provide direction for further structural modifications to improve activity. In this article, we present data that suggest the activity of antitrypanosomal dihydroquinolines is through induction of oxidative stress. We rationalize that the potency and selectivity of this series of compounds are based on the limited ROS-scavenging capacity of the parasite’s redox system and/or peculiarities in the redox status of trypanosomes compared to host cells (16–18, 21, 31, 34).

We hypothesized that parasites with reduced expression of ROS-detoxifying enzymes would offer the opportunity to test our idea that antitrypanosomal dihydroquinolines act through inducing oxidative stress. For these experiments, we used an inducible RNAi system to independently knock down the ROS-detoxifying enzymes TbTryS and TbSODB, thus creating parasites with a compromised ROS detoxification system. We selected these enzymes on the basis of their proven essentiality using both chemical and genetic approaches (1, 7, 27, 32, 40, 41). TbTryS has been

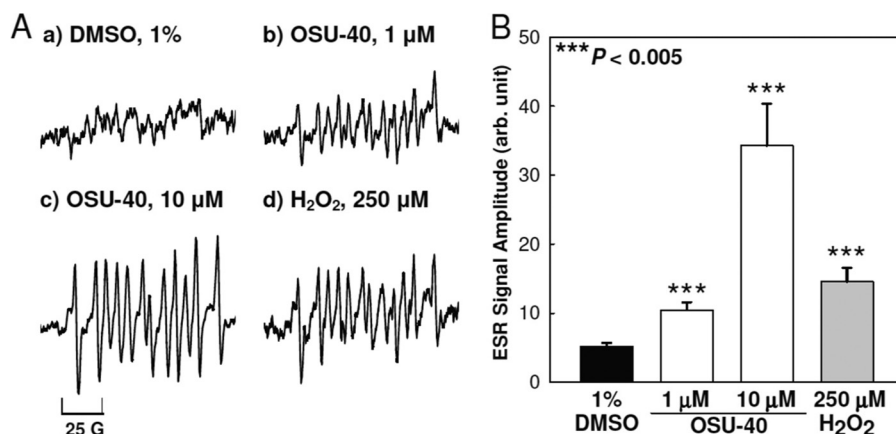


FIG 4 ESR spectra and signal quantification in trypanosomes exposed to OSU-40. (A) ESR spectra observed after incubation of bloodstream form *T. b. brucei* 221 cells with DMSO (1%) (a), OSU-40 (1 μ M) (b), OSU-40 (10 μ M) (c), and H₂O₂ (250 μ M) (d). (B) Quantification of ESR signals. Results are means \pm standard deviations (SD) from three independent experiments. Asterisks (***) ($P < 0.005$) indicate statistically significant differences between the DMSO-treated group and the treatment groups as assessed by Student's *t* test.

validated as a drug target using small molecule inhibitors (32), and TbSODB-null parasites show increased sensitivity to the superoxide-generating molecules paraquat and nifurtimox (27). In our experiments, an increased susceptibility to OSU-40 was observed upon knockdown of either TbTryS or TbSODB, consistent with the hypothesis that antitrypanosomal dihydroquinolines induce oxidative stress in the parasite.

We observed a more dramatic increase in susceptibility to OSU-40 in TbSODB RNAi parasites (3.4-fold) compared to the results with TbTryS RNAi parasites (2.4-fold). Reduced expression of TbSODB would be expected to lead to rapid accumulation of superoxide anion within the trypanosome, considering that TbSODs are the only enzymes responsible for detoxifying this highly toxic radical in the parasite. However, RNAi-mediated knockdown of TbTryS was previously reported to increase expression of *T. brucei* trypanothione reductase (TbTryR), γ -glutamyl-cysteine synthetase (Tb γ -GCS), and ornithine decarboxylase (TbODC) (1). It is possible that the upregulation of these enzymes could serve to maintain a favorable intracellular redox potential and lead to less dramatic effects on both growth rate and OSU-40 susceptibility in TbTryS RNAi-induced parasites. In addition to work with TbTryS and TbSODB, we generated parasites harboring a TbSODA RNAi targeting construct. While 6-fold-lower mRNA levels were observed 3 days after the addition of tetracycline, neither the growth rate nor the susceptibility to OSU-40 was affected in TbSODA RNAi organisms (data not shown). A possible explanation for these observations may be that TbSODB could compensate for the loss of TbSODA in the TbSODA RNAi-induced parasites.

We have also shown direct evidence through ESR spectroscopy that the dihydroquinoline OSU-40 induces free radical formation. ESR (also known as electron paramagnetic resonance [EPR]) spectroscopy detects paramagnetic species in an external magnetic field, where the paramagnetic species absorb microwave energy leading to the transition of spin states (19, 37). Spin trapping allows the detection of radicals by ESR spectroscopy through the formation of radical adducts between the spin trapping reagent and free radicals. The technology has been used in chemical systems and increasingly in biomedical applications, including the

measurement of free radical formation in trypanosomatids and other biological systems (6, 23, 26, 37). In this study, inclusion of 1 μ M OSU-40 in trypanosome cultures resulted in a clear ESR signal in as little as 30 min (data not shown). Also, a dose-dependent production of signals corresponding to free radical species was observed after treating the parasites with OSU-40 for 60 min. These data are consistent with our previous experiments showing increased fluorescence when trypanosomes were incubated with the redox active dye CM-H₂DCFDA in the presence of OSU-40 (11). The spectra recorded after treatment of trypanosomes with OSU-40 and H₂O₂ showed identical ESR features, which suggest the radicals are carbon centered in both cases and possibly produced by the same mechanism. However, we do not know if this represents initial or end products and whether the initial products are different in the two cases.

A pharmacokinetic study of OSU-40 and OSU-36-HCl in rats showed that OSU-40 was rapidly converted to OSU-36 in plasma, with OSU-36 subsequently undergoing oxidative metabolism (12). Together with the results obtained here, we propose the following addition to the proposed mode of action of antitrypanosomal dihydroquinolines (11) (Fig. 5): compounds esterified at the 6-oxygen atom are hydrolyzed by esterases and then oxidized to the corresponding quinone imine species spontaneously. Redox cycling between the quinone imine and semiquinone radical results in the generation of superoxide. Trypanothione reductase has been reported to catalyze the reduction of quinones (5, 13, 30) and could facilitate the initiation of single-electron redox cycling. Hydrogen peroxide and hydroxyl radical formed as a consequence of superoxide production (15, 33, 34) together with superoxide would lead to *T. brucei* parasite cell death.

A central issue regarding reagents inducing oxidative stress is selectivity. Although increased levels of ROS are certainly toxic to a pathogen such as *T. brucei*, excessive amounts of these reactive species can be toxic to the host due to their high reactivity with biological molecules such as DNA, protein, and lipids. However, selectivity can be achieved through different manipulation of vulnerability to oxidative stress. For example, targeting the ROS stress response has been proposed as a strategy to selectively kill cancer cells (28, 33, 35). The small molecule piperlongumine was

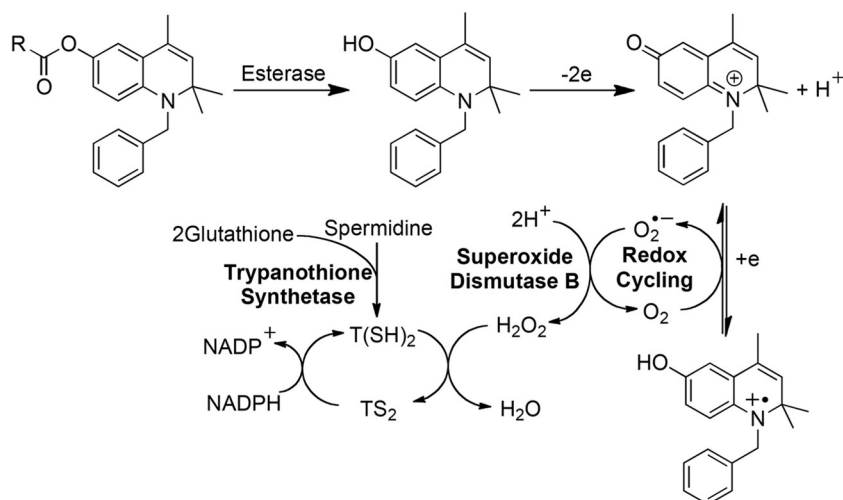


FIG 5 Proposed mode of action for generation of oxidative stress by the antitrypanosomal dihydroquinolines, including the possible protective role of TbTryS and TbSODB. In this model, dihydroquinolines such as OSU-40 are hydrolyzed by an esterase activity followed by auto-oxidation. The resulting quinone imine can then undergo redox cycling, leading to oxidative stress. The results of this investigation suggest that the parasite's antioxidant enzymes trypanothione synthetase and superoxide dismutase B are utilized to lessen the toxic effects of this class of antitrypanosomal agents.

recently reported to lead to apoptotic cell death in cancer cells by increasing the level of ROS (28). An altered redox status appears to make cancer cells more vulnerable to oxidative stress, providing the basis for selectivity of this novel chemotherapeutic strategy (28, 33, 35). In the case of trypanosomatids, ROS generation has been widely studied as a mechanism for drugs targeting *T. cruzi*. In fact, the two agents used clinically for treating American trypanosomiasis, nifurtimox and benznidazole, are both suggested to induce free radical formation (8–10, 21). The selectivity of ROS-generating reagents for trypanosomatids over host cells might be explained by the unique biochemical features of these parasites, particularly their peculiar ROS-scavenging system based on trypanothione-dependent peroxidases (16–18, 21, 31, 34). Trypanosomatids also lack glutathione reductase, thioredoxin reductase, catalase, and selenium-containing glutathione peroxidases, possibly making them deficient in defense against oxidative stress. Fairlamb et al. proposed that the essential parasite enzymes trypanothione synthetase (32, 41) and trypanothione reductase (24, 25) are promising drug targets and reported different classes of small molecule inhibitors (24, 25, 32) that interfere with the ROS-scavenging system. Taken together, these studies support the idea that the induction of oxidative stress can be an effective strategy for developing antitrypanosomal agents.

In conclusion, we have demonstrated that decreased expression of the key trypanosome antioxidant enzymes TbTryS and TbSODB results in an increased susceptibility of bloodstream-form *T. brucei* to the representative dihydroquinoline OSU-40. We have also used ESR spectroscopy to directly detect the formation of free radicals upon exposure of *T. brucei* to OSU-40. These data strongly support that the mode of antitrypanosomal action for this class of compounds is to induce oxidative stress. Validation of the induction of oxidative stress as the mode of action for dihydroquinolines may open the door for new therapeutic strategies targeting African trypanosomiasis.

ACKNOWLEDGMENTS

We thank James Morris (Clemson University, Clemson, SC) for providing genomic DNA, the RNAi vector, and the 90-13 strain of *T. b. brucei*. We

also thank Alan Fairlamb (University of Dundee, Scotland, United Kingdom) for providing TryS antiserum and Paul Michels (Catholic University of Louvain, Brussels, Belgium) for providing α -enolase antiserum. Stephen Hajduk and Rudo Kieft (University of Georgia, Athens) are acknowledged for sharing protocols.

REFERENCES

1. Ariyanayagam MR, Oza SL, Guther MLS, Fairlamb AH. 2005. Phenotypic analysis of trypanothione synthetase knockdown in the African trypanosome. *Biochem. J.* 391:425–432.
2. Barrett MP, Boykin DW, Brun R, Tidwell RR. 2007. Human African trypanosomiasis: pharmacological re-engagement with a neglected disease. *Br. J. Pharmacol.* 152:1155–1171.
3. Burkard G, Fragoso CM, Roditi I. 2007. Highly efficient stable transformation of bloodstream forms of *Trypanosoma brucei*. *Mol. Biochem. Parasitol.* 153:220–223.
4. Burri C. 2010. Chemotherapy against human African trypanosomiasis: is there a road to success? *Parasitology* 137:1987–1994.
5. Cenas N, Arscott D, Williams C, Jr, Blanchard J. 1994. Mechanism of reduction of quinones by *Trypanosoma congolense* trypanothione reductase. *Biochemistry* 33:2509–2515.
6. Cerecetto H, et al. 1999. 1,2,5-Oxadiazole N-oxide derivatives and related compounds as potential antitrypanosomal drugs: structure-activity relationships. *J. Med. Chem.* 42:1941–1950.
7. Comini MA, et al. 2004. Validation of *Trypanosoma brucei* trypanothione synthetase as drug target. *Free Radic. Biol. Med.* 36:1289–1302.
8. Docampo R, Moreno SNJ. 1984. Free radical metabolites in the mode of action of chemotherapeutic agents and phagocytic cells on *Trypanosoma cruzi*. *Rev. Infect. Dis.* 6:223–238.
9. Docampo R, et al. 1981. Mechanism of nifurtimox toxicity in different forms of *Trypanosoma cruzi*. *Biochem. Pharmacol.* 30:1947–1951.
10. Docampo R, Stoppani AOM. 1979. Generation of superoxide anion and hydrogen peroxide induced by nifurtimox in *Trypanosoma cruzi*. *Arch. Biochem. Biophys.* 197:317–321.
11. Fotie J, et al. 2010. Antitrypanosomal activity of 1,2-dihydroquinolin-6-ols and their ester derivatives. *J. Med. Chem.* 53:966–982.
12. Gershkovich P, et al. 2011. Simultaneous determination of a novel antitrypanosomal compound (OSU-36) and its ester derivative (OSU-40) in plasma by HPLC: application to first pharmacokinetic study in rats. *J. Pharm. Pharm. Sci.* 14:36–45.
13. Henderson G, et al. 1988. "Subversive" substrates for the enzyme trypanothione disulfide reductase: alternative approach to chemotherapy of Chagas disease. *Proc. Natl. Acad. Sci. U. S. A.* 85:5374–5378.
14. Hirumi H, Hirumi K. 1989. Continuous cultivation of *Trypanosoma*

- brucei* blood stream forms in a medium containing a low concentration of serum protein without feeder cell layers. *J. Parasitol.* 75:985–989.
15. Imlay JA. 2003. Pathways of oxidative damage. *Annu. Rev. Microbiol.* 57:395–418.
 16. Jaeger T, Flohe L. 2006. The thiol-based redox networks of pathogens: unexploited targets in the search for new drugs. *Biofactors* 27:109–120.
 17. Krauth-Siegel RL, Comini MA. 2008. Redox control in trypanosomatids, parasitic protozoa with trypanothione-based thiol metabolism. *Biochim. Biophys. Acta* 1780:1236–1248.
 18. Krauth-Siegel RL, Meiering SK, Schmidt H. 2003. The parasite-specific trypanothione metabolism of trypanosoma and leishmania. *Biol. Chem.* 384:539–549.
 19. Kuppusamy P. 2004. EPR spectroscopy in biology and medicine. *Antioxid. Redox Signal.* 6:583–585.
 20. Livak KJ, Schmittgen TD. 2001. Analysis of relative gene expression data using real-time quantitative PCR and the 2^{(-Delta Delta C(T))} method. *Methods* 25:402–408.
 21. Maya JD, et al. 2007. Mode of action of natural and synthetic drugs against *Trypanosoma cruzi* and their interaction with the mammalian host. *Comp. Biochem. Physiol. A Mol. Integr. Physiol.* 146:601–620.
 22. Opigo J, Woodrow C. 2009. NECT trial: more than a small victory over sleeping sickness. *Lancet* 374:7–9.
 23. Otero L, et al. 2006. Novel antitrypanosomal agents based on palladium nitrofurylthiosemicarbazone complexes: DNA and redox metabolism as potential therapeutic targets. *J. Med. Chem.* 49:3322–3331.
 24. Patterson S, et al. 2011. Dihydroquinazolines as a novel class of *Trypanosoma brucei* trypanothione reductase inhibitors: discovery, synthesis, and characterization of their binding mode by protein crystallography. *J. Med. Chem.* 54:6514–6530.
 25. Perez-Pineiro R, et al. 2009. Development of a novel virtual screening cascade protocol to identify potential trypanothione reductase inhibitors. *J. Med. Chem.* 52:1670–1680.
 26. Porcal W, et al. 2008. New trypanocidal hybrid compounds from the association of hydrazone moieties and benzofuroxan heterocycle. *Bioorg. Med. Chem.* 16:6995–7004.
 27. Prathalingham SR, Wilkinson SR, Horn D, Kelly JM. 2007. Deletion of the *Trypanosoma brucei* superoxide dismutase gene *sodB1* increases sensitivity to nifurtimox and benznidazole. *Antimicrob. Agents Chemother.* 51:755–758.
 28. Raj L, et al. 2011. Selective killing of cancer cells by a small molecule targeting the stress response to ROS. *Nature* 475:231–234.
 29. Reid CS, et al. 2011. Synthesis and antitrypanosomal evaluation of derivatives of N-benzyl-1,2-dihydroquinolin-6-ols: effect of core substitutions and salt formation. *Bioorg. Med. Chem.* 19:513–523.
 30. Salmon-Chemin L, et al. 2001. 2- and 3-substituted 1,4-naphthoquinone derivatives as subversive substrates of trypanothione reductase and lipamide dehydrogenase from *Trypanosoma cruzi*: synthesis and correlation between redox cycling activities and in vitro cytotoxicity. *J. Med. Chem.* 44:548–565.
 31. Schmidt A, Krauth-Siegel RL. 2002. Enzymes of the trypanothione metabolism as targets for antitrypanosomal drug development. *Curr. Top. Med. Chem.* 2:1239–1259.
 32. Torrie LS, et al. 2009. Chemical validation of trypanothione synthetase: a potential drug target for human trypanosomiasis. *J. Biol. Chem.* 284:36137–36145.
 33. Trachootham D, Alexandre J, Huang P. 2009. Targeting cancer cells by ROS-mediated mechanisms: a radical therapeutic approach? *Nat. Rev. Drug Discov.* 8:579–591.
 34. Turrens JF. 2004. Oxidative stress and antioxidant defenses: a target for the treatment of diseases caused by parasitic protozoa. *Mol. Aspects Med.* 25:211–220.
 35. Verrax J, et al. 2011. Redox-active quinones and ascorbate: an innovative cancer therapy that exploits the vulnerability of cancer cells to oxidative stress. *Anticancer Agents Med. Chem.* 11:213–221.
 36. Villamena FA, Hadad CM, Zweier JL. 2003. Kinetic study and theoretical analysis of hydroxyl radical trapping and spin adduct decay of alkoxy-carbonyl and dialkoxyphosphoryl nitrones in aqueous media. *J. Phys. Chem. A* 107:4407–4414.
 37. Villamena FA, Zweier JL. 2004. Detection of reactive oxygen and nitrogen species by EPR spin trapping. *Antioxid. Redox Signal.* 6:619–629.
 38. Wang ZF, Morris JC, Drew ME, Englund PT. 2000. Inhibition of *Trypanosoma brucei* gene expression by RNA interference using an integratable vector with opposing T7 promoters. *J. Biol. Chem.* 275:40174–40179.
 39. WHO. 23 May 2011, posting date. New cases of African trypanosomiasis continue to drop. World Health Organization, Geneva, Switzerland. http://www.who.int/neglected_diseases/disease_management/HAT_cases_drop/en/index.html.
 40. Wilkinson SR, et al. 2006. Functional characterisation of the iron superoxide dismutase gene repertoire in *Trypanosoma brucei*. *Free Radic. Biol. Med.* 40:198–209.
 41. Wyllie S, et al. 2009. Dissecting the essentiality of the bifunctional trypanothione synthetase-amidase in *Trypanosoma brucei* using chemical and genetic methods. *Mol. Microbiol.* 74:529–540.
 42. Yun O, Priotto G, Tong J, Flevaud L, Chappuis F. 2010. NECT is next: implementing the new drug combination therapy for *Trypanosoma brucei gambiense* sleeping sickness. *PLoS Negl. Trop. Dis.* 4:e720.